



# Early Enhancement in Breast DCE-MRI is Sparse and can be Imaged with Reduced FOV to Increase Temporal Resolution

F. Pineda, T. Easley, G. Karczmar

Department of Radiology, The University of Chicago, Chicago, IL

## Key points

- **Shortly after contrast dye is administered to a patient, breast MRIs enhance sparsely**
- **Progressively aliased images taken shortly after contrast administration can be ‘unfolded’ to reconstruct full-field of view (FOV) images**
- **Acquiring aliased images offers higher time resolutions to ‘ultrafast’ DCE-MRI protocols, which have shown potential advantages in identifying and classifying breast tumors**

## Background

‘Ultrafast’ imaging in dynamic contrast-enhanced (DCE) MRI has recently shown advantages over standard protocols in initial imaging<sup>1,2</sup>: tumors are more conspicuous and early-time contrast uptake can be more precisely quantified, aiding lesion classification and differentiation.

In the first 30-45 seconds after injection, on average, less than 7% of the FOV showed significant enhancement. This suggests a possibility for faster acquisitions: reduce the FOV and allow aliasing. Since early enhancement is sparse, few voxels are likely to overlap and full-FOV images can be closely approximated by ‘unfolding’ and filtering aliased images.

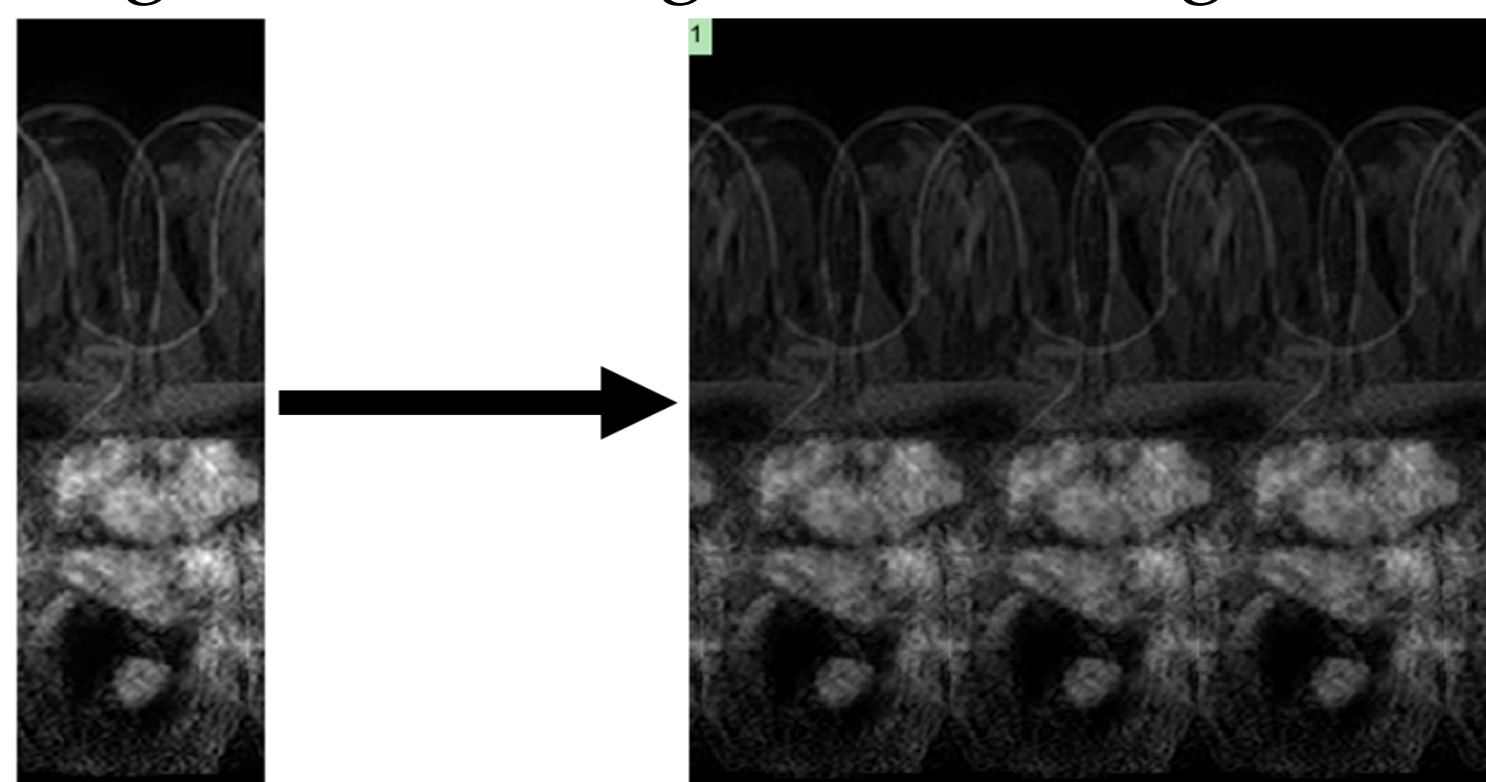


**Figure 1.** An aliased image acquired at 31% of full FOV is unfolded.

## References

- [1]Pineda et al. Acad Radiol 2016;23(9):1137-1144.  
[2]Abe et al. AJR Am J Roentgenol 2016;207(5):1159-1166  
[3]Mehul et al. IEEE Transactions on Image Processing, 2009;18(11):2385-2401

## Algorithm and Methodology

Five patients imaged with an ultrafast DCE protocol with marked background parenchymal enhancement and enhancing lesions were selected. These five image sets had the highest density of enhancing voxels and offered the lowest odds of a successful reconstruction from aliased images.

Aliasing was simulated for the first three post-contrast time-points at a set of progressively increasing reduced FOVs: 31%, 44%, and 77% of the initial FOV. These reduction factors were chosen to minimize the number of overlaps in lesions in the images, and the resulting reconstructions were compared against other increasing FOV combinations with the same average reduction.

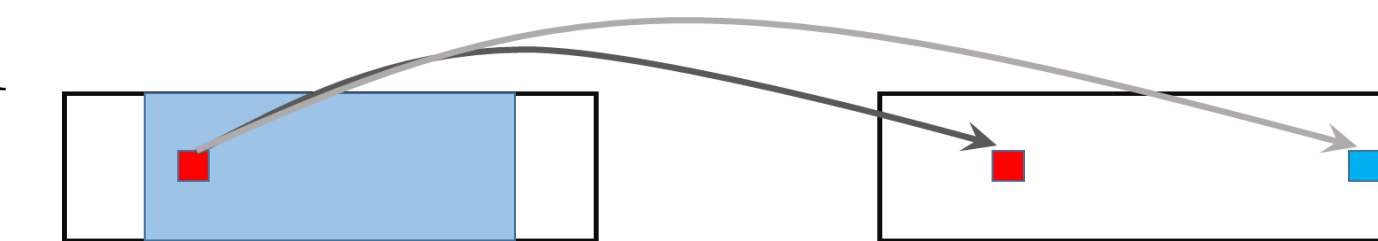


**Figure 2.** Each enhancing voxel that could have aliased in the reduced FOV image was copied to the corresponding location(s) in the full-FOV that also enhanced in the reference image(s).

The correct location of each significantly enhancing voxel (signal increase above a noise threshold) was selected based on comparison of the aliased images with later images. Each reduced FOV copied an enhancing voxel to a different set of aliases. Voxels that did not enhance at all time-points after first appearance were removed from the image. Voxels that overlap (share a set of aliases in at least one time point) were interpolated in time.

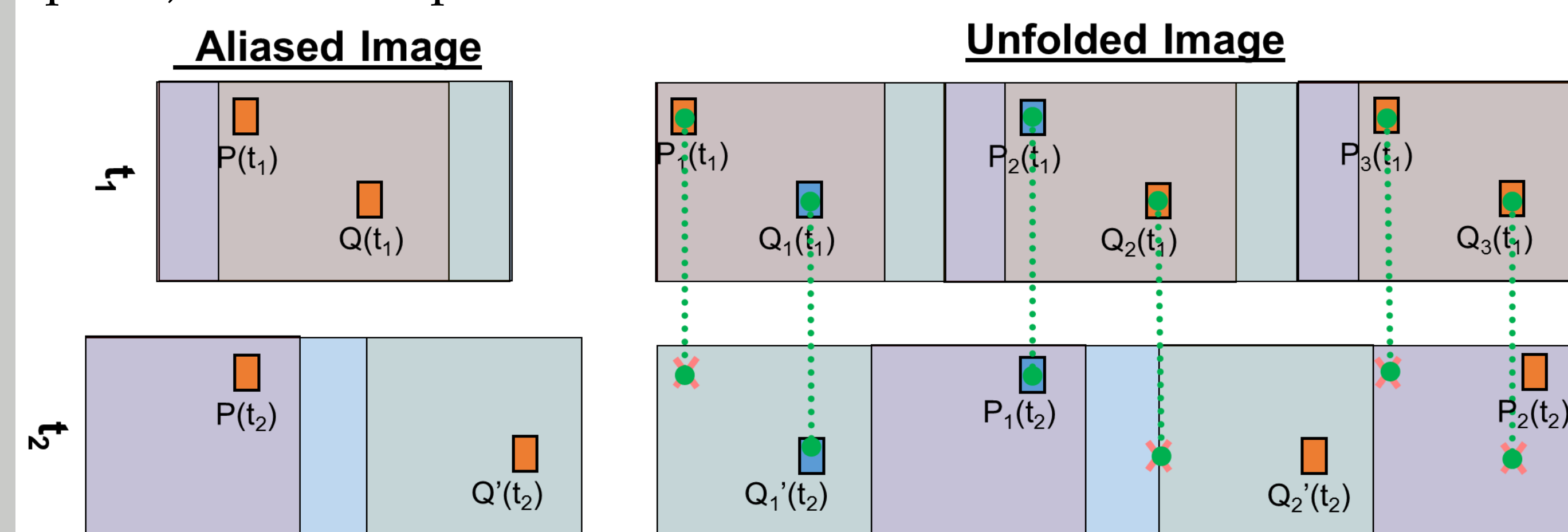


**Figure 3.** Diagram of aliased images acquired with a progressively increasing FOV. Because FOVs vary over time, each enhancing voxel will be copied to sets of points that agree only on a single location at all subsequent times.

Image similarity between the original and reconstructed images was evaluated using the complex wavelet structural similarity index metric (CW-SSIM)<sup>3</sup>. Reconstructions from varying combinations of FOVs were compared by mean CW-SSIM.

## Results and Conclusions

An average of 2.5% (range 0-6.6%) of the enhancing voxels above the chest wall overlapped in reconstructed images. These unfolded images had CW-SSIM numbers of 0.64, 0.93, and 0.97. Progressive aliasing and unfolding led to images that were very similar to fully-sampled images and could be acquired with a temporal resolution as low as 2 seconds.

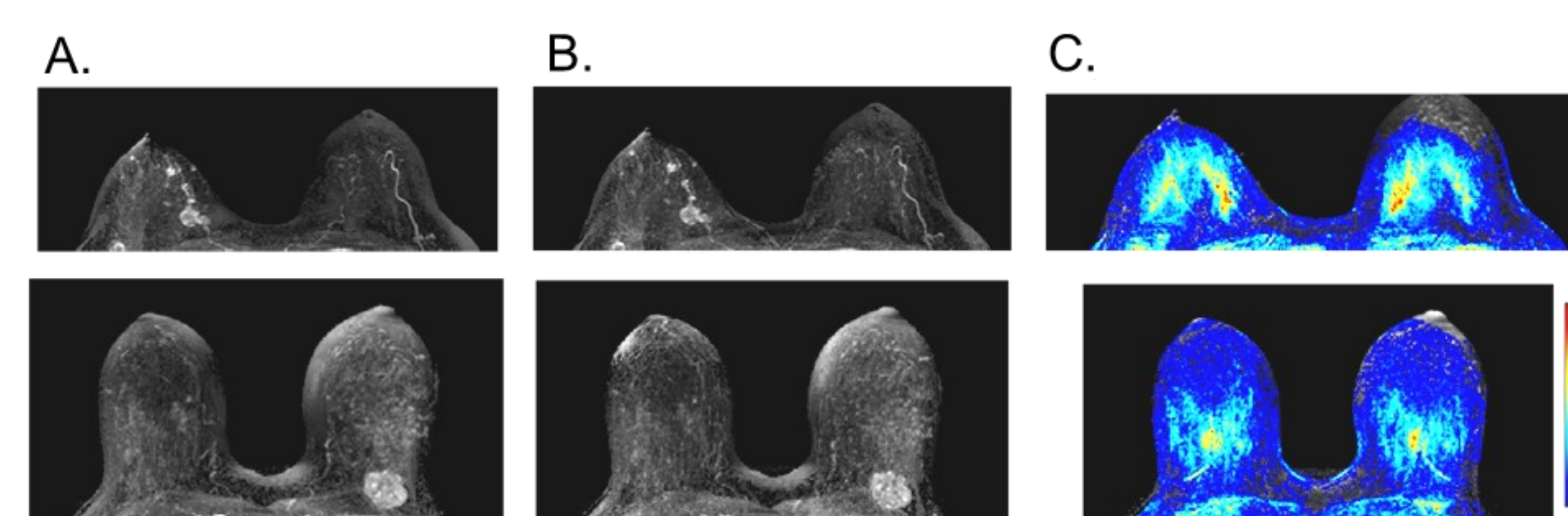


**Figure 6.** Examples from two of the simulations: **A.** Original maximum intensity projections (MIPs) of difference images; **B.** MIPs reconstructed from progressive aliasing at 44% of the FOV; **C.** Color maps showing the number of real overlaps (summed over 120 slices and 3 time-points) per pixel.

We have not yet found a case-independent strategy for optimizing factor selection. Choosing increasing coprime factors (those whose products with image width are coprime integers) near  $(\text{avgfactor} \cdot \frac{3}{5}) \cdot (1,2,2)$  gave the best CW-SSIM for most image sets, but failed to preserve lesions in some cases.

## Comparing Fields of View

Varying distributions of FOV reduction produce reconstructions of varying quality. All viable factor triplets were used to simulate aliasing and unfolding for each case. Viable triplets were all ordered 3-odd-integer partitions of  $3 \cdot \text{avgfactor} \cdot \text{FOVwidth}$  (in pixels). CW-SSIM values were calculated for each triplet.

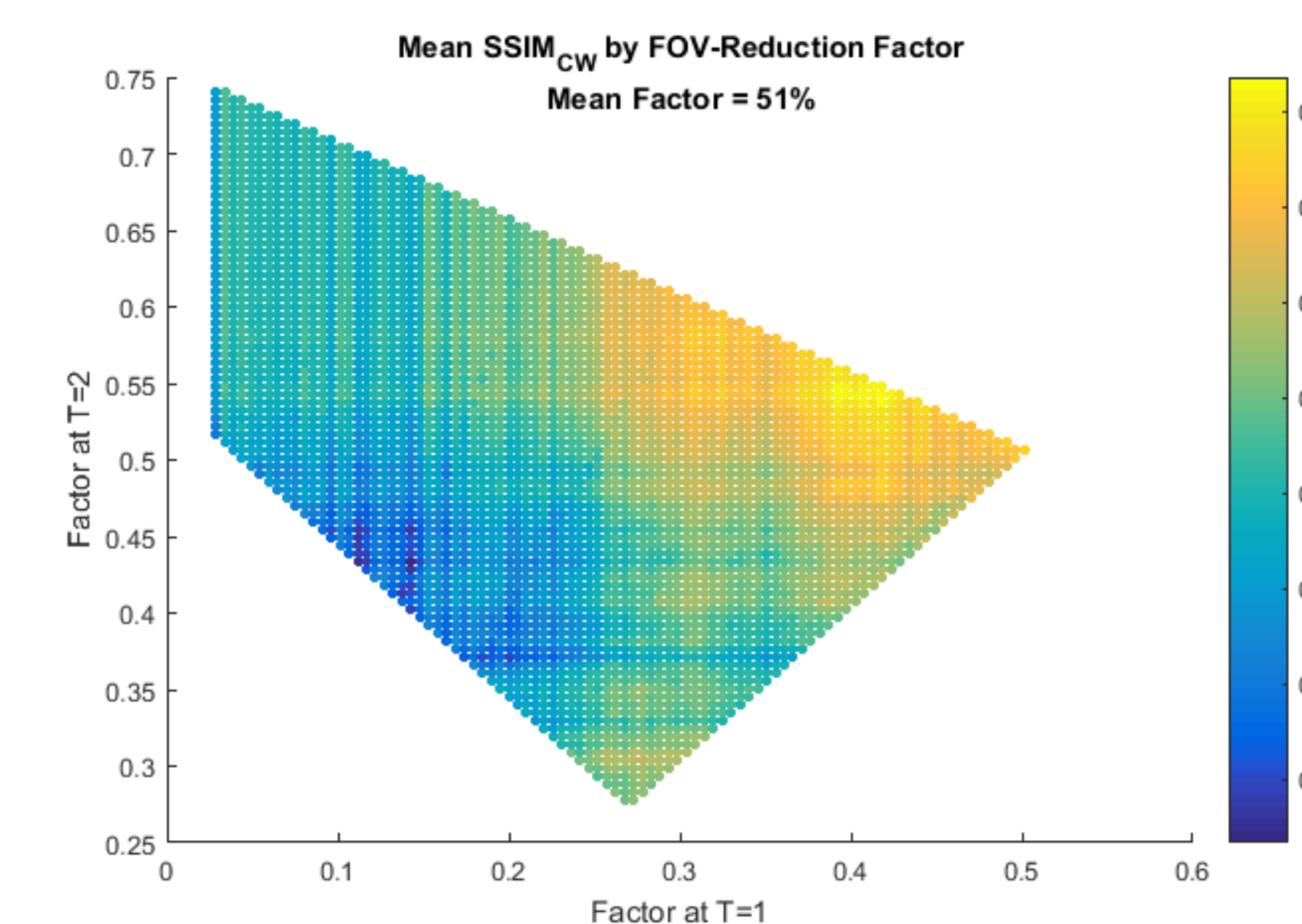


**Figure 4.** One case's color map of image similarity as a function of FOV reduction per time-point. CW-SSIM is averaged over the whole image set at each factor.

## Parallelization and Scalability

Because each parallel worker only needs a list of FOV-reduction factors and the initial image set, this is an “embarrassingly parallel problem.” Each factor triplet is assigned to a worker that simulates aliasing, unfolds the resulting images, and assesses the quality of the image reconstruction. When using multiple workers, neither the number of workers nor assignments had a significant effect on average assignment time. Running multiple workers extended average assignment time by ~18%. The tests plotted below ran on bigmem2 in Midway.

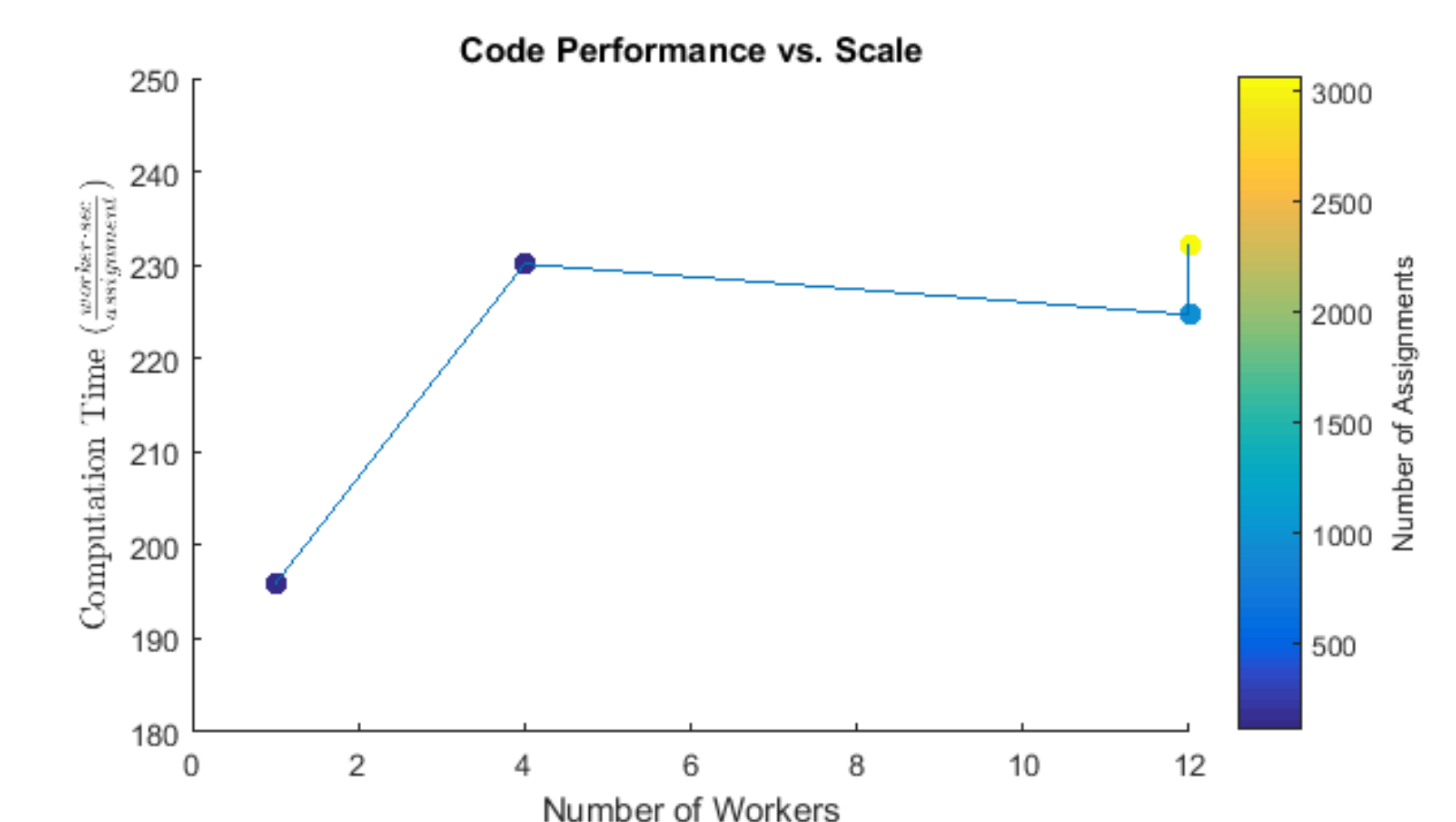


**Figure 5.** Computing time was calculated as (runtime)\*(number of workers)/(number of assignments), and appears to be relatively insensitive to increases in either the number of workers or the total number of assignments when running on multiple workers.